

Spontaneous spin-lattice coupling in the geometrically frustrated triangular lattice antiferromagnet CuFeO_2

F. Ye,¹ Y. Ren,² Q. Huang,³ J. A. Fernandez-Baca,^{1,4} Pengcheng Dai,^{4,1} J. W. Lynn,³ and T. Kimura⁵

¹Center for Neutron Scattering, Oak Ridge National Laboratory, Oak Ridge, Tennessee 37831-6393, USA

²X-ray Science Division, Argonne National Laboratory, Argonne, Illinois 60439, USA

³NIST Center for Neutron Research, National Institute of Standards and Technology, Gaithersburg, Maryland 20899, USA

⁴Department of Physics and Astronomy, The University of Tennessee, Knoxville, Tennessee 37996-1200, USA

⁵Los Alamos National Laboratory, Los Alamos, New Mexico 87545, USA

(Received 10 May 2006; published 22 June 2006)

We use high-resolution synchrotron x-ray and neutron diffraction to study the geometrically frustrated triangular lattice antiferromagnet CuFeO_2 . On cooling from room temperature, CuFeO_2 undergoes two antiferromagnetic phase transitions with incommensurate and commensurate magnetic order at $T_{N1}=14$ K and $T_{N2}=11$ K, respectively. The occurrence of these two magnetic transitions is accompanied by second- and first-order structural phase transitions from hexagonal to monoclinic symmetry. Application of a 6.9 T magnetic field lowers both transition temperatures by ~ 1 K, and induces an additional incommensurate structural modulation in the temperature region where the field-driven ferroelectricity occurs. These results suggest that a strong magneto-elastic coupling is intimately related to the multiferroic effect.

DOI: [10.1103/PhysRevB.73.220404](https://doi.org/10.1103/PhysRevB.73.220404)

PACS number(s): 75.30.Kz, 64.70.Rh, 75.25.+z

Frustrated spin systems have recently attracted considerable attention because of their novel magnetic and multiferroic properties.¹⁻³ The frustration is caused by either competing interactions or lattice geometries, which disallow the energy minimization of all spin pairs simultaneously, thus leading to a large number of degenerate spin configurations. In principle, a strongly frustrated system should exhibit no long-range spin order.^{4,5} However, magnetic frustration can often be lifted by a symmetry-reducing lattice distortion at finite temperature and therefore allow long-range magnetic order at lower temperatures.^{6,7} Similarly, application of a magnetic field can also release the spin frustration and, in some cases, induce electric polarization.^{1,2,8} Since the original theoretical prediction and experimental observation of a magnetoelectric effects,^{9,10} there has been continued efforts to study materials with strong interplay between magnetism and ferroelectricity.¹¹ The quasi-two-dimensional (2D) triangular lattice antiferromagnet (TLA) CuFeO_2 is one of a few materials with a novel magnetoelectric effect under modest magnetic field. It has been proposed that a noncollinear magnetic structure such as a spiral state will induce electric polarization.¹¹ In this paper, we report x-ray and neutron diffraction studies of the magnetic and structural properties of CuFeO_2 . We show that the antiferromagnetic (AF) transitions in CuFeO_2 are accompanied simultaneously by structural phase transitions from hexagonal (space group $R\bar{3}m$) to monoclinic (space group $C2/m$). Furthermore, application of a magnetic field that brings about ferroelectricity also induces a structural modulation, thus providing direct evidence for the strong spin-lattice coupling in this 2D geometrically frustrated TLA.

The TLA is the simplest example of geometrically spin frustrated systems.¹²⁻¹⁴ A typical spin ordering in a TLA is the 120° structure where the three spins align at 120° to each other in the basal plane with two types of chirality.^{6,12} As a prototype for 2D TLA systems, the delafossite compound CuFeO_2 has been extensively investigated.¹⁵⁻¹⁷ The compound has a layered structure of triangular lattices of Fe^{3+}

ions [see Figs. 1(a)–1(c)]. Previous neutron diffraction measurements suggest that this system undergoes successive AF phase transitions.¹⁸ At $T_{N1}=14$ K, the sample first enters into a partially disordered, incommensurate (IC) magnetic state with sinusoidal spin amplitude. Upon further cooling to $T_{N2}=11$ K, a collinear and commensurate (C) $\uparrow\uparrow\downarrow$ (four-sublattice) spin structure forms in the Fe^{3+} plane, in contrast to the noncollinear three-sublattice 120° magnetic structure. With increasing magnetic field along the c axis, the system exhibits multistep metamagnetic phase transitions.^{19,20} Although the Fe^{3+} magnetic ions in CuFeO_2 are essentially classical Heisenberg spins with an orbital singlet, exchange coupling up to third nearest neighbors has to be considered to account for the magnetic structure within the 2D Ising spin TLA model.¹⁸ The reason for the unusually large second- and third-nearest-neighbor interactions in comparison with the nearest-neighbor coupling ($J_2/J_1=0.45$ and $J_3/J_1=0.75$) is not understood.²⁰ Moreover, recent investigations on the magnetoelectric and magnetoelastic properties of the CuFeO_2 system reveal that the successive magnetic transitions are accompanied by magnetoelectric phase transitions as well as drastic lattice distortions.²¹ To understand the microscopic origin of the unusual spin structure and the observed multiferroic properties in CuFeO_2 , we carried out a detailed structural and magnetic investigation using high-resolution synchrotron x-ray and neutron diffraction techniques.

A polycrystalline specimen of CuFeO_2 was prepared using conventional solid state reaction methods with mixtures of Cu_2O and Fe_2O_3 and single-crystal specimens were grown by the floating zone method. High-resolution, high-energy (115 keV) synchrotron x-ray scattering measurements were performed at the 11-ID-C station, Advanced Photon Source, Argonne National Laboratory. High-resolution neutron powder diffraction (NPD) patterns were collected on the high-resolution, 32-counter BT-1 diffractometer at the NIST Center for Neutron Research (NCNR). The measurements on the single crystal sample were carried out at the HB3 triple-axis

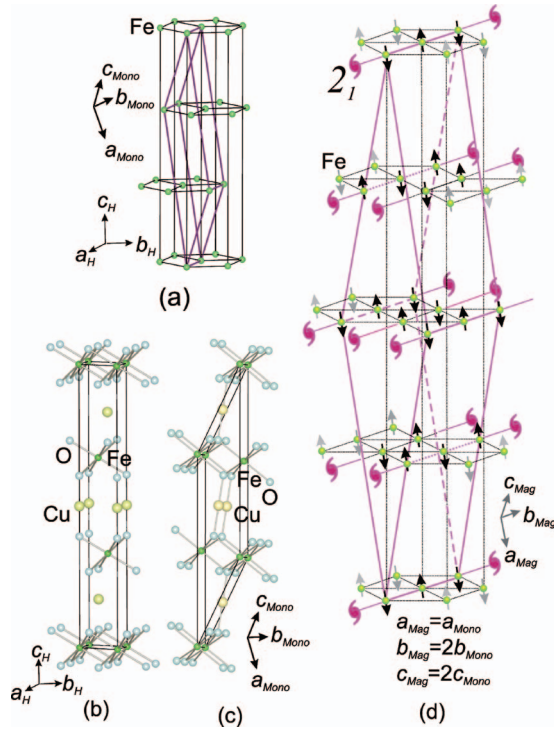


FIG. 1. (Color) (a) Relation between the high- T hexagonal and low- T monoclinic structures. Unit cell of (b) the hexagonal structure (space group $R\bar{3}m$), (c) the monoclinic lattice structure (space group $C2/m$), and (d) the monoclinic magnetic structure. Spin orientations are also labeled.

spectrometer at the High-Flux Isotope Reactor (HFIR), Oak Ridge National Laboratory.

In Fig. 2(a), synchrotron x-ray diffraction patterns show the splitting of the (110) peak in hexagonal symmetry as the system crosses the two Néel temperatures. When the temperature drops below $T_{N1}=14$ K, the peak becomes asymmetric, indicating a splitting due to a lattice distortion to a lower symmetry. The sudden splitting of the (110) peak into two well-resolved peaks at $T < T_{N2}=11$ K suggests a first-order structural phase transition induced by the magnetic transition. To correlate the lattice response with the magnetic properties, we collected field-dependent neutron data in this temperature region. As shown in Fig. 2(b), the IC AF structure has a magnetic superlattice peak with propagation wave vector $\vec{\tau}=(q, q, 1.5)$ below T_{N1} , where q increases from 0.19 to 0.22 with decreasing temperature. At T_{N2} , a collinear, commensurate magnetic structure sets in and the intensity increases sharply.^{18,22} There is significant hysteresis in the magnetic peak intensity around T_{N2} accompanied by a clear structural phase transition. In contrast, the magnetic phase transition around T_{N1} shows no observable hysteresis. This suggests that the magnetic phase transitions at T_{N1} and T_{N2} are second and first order, respectively. We notice that lattice modulations at $(q, q, 0)$ in the synchrotron x-ray measurements correlate nicely with the magnetic wave vector [Fig. 2(d)]. After we applied a magnetic field of 6.9 T along the c axis (in hexagonal notation), both the IC-C magnetic and structural phase transitions (revealed by the change of lattice modulation) are clearly suppressed from 11 K to lower tem-

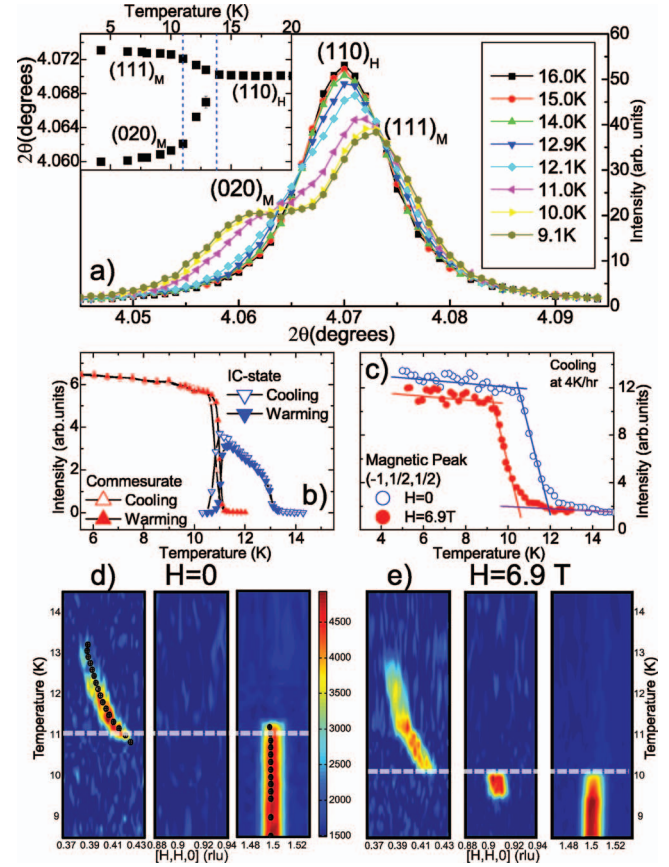


FIG. 2. (Color) (a) Synchrotron x-ray diffraction patterns showing the hexagonal (110) peak splitting to two peaks with decreasing temperature. The inset shows the temperature dependence of the peak splitting obtained from fits. (b) Temperature dependence of the integrated intensities of the incommensurate $(q, q, 1.5)$ and the commensurate $(1/4, 1/4, 1.5)$ magnetic peaks, respectively, from neutron scattering. (c) Magnetic intensities as a function of temperature in zero field (open) and $H=6.9$ T (solid). The lines are guides to the eye. Temperature dependence of selected structural modulations in (d) zero field and (e) $H=7$ T. Solids circles show predicted lattice modulation wave vector \vec{q}_l according to the relation $\vec{q}_l=2\vec{q}_s$, where \vec{q}_s is the magnetic modulation wave vector.

peratures. Such observations demonstrate that the structural transitions are indeed induced by the magnetic ordering. In addition, in the temperature region where the magnetic-field-induced electric polarization occurs,²¹ an extra incommensurate lattice modulation is found at wave vector $\vec{\tau}=(0.91, 0.91, 0)$ [Fig. 2(e)], consistent with the previously reported incommensurate magnetic structure.²³ These results indicate that the lattice distortion is directly related to the magnetic-ferroelectric behavior.

From the high-resolution synchrotron x-ray and NPD data, we find that the low-temperature crystal structure has monoclinic symmetry with space group $C2/m$. The relation between the hexagonal and the monoclinic lattices is depicted in Figs. 1(a)–1(c). The hexagonal $R\bar{3}m$ and monoclinic $C2/m$ symmetries were used for the nuclear structure at temperatures above T_{N1} and below T_{N2} , respectively. Earlier neutron diffraction measurements on powder and single crystals assumed that the cell parameters remained un-

TABLE I. Structural parameters of CuFeO_2 at 4 and 17 K. Atomic positions for the $R\bar{3}m$ symmetry are, for Cu, $3a(0,0,0)$, Fe, $3b(0,0.5,0)$, and O, $6c(0,0,z)$, and for $C2/m$ symmetry Cu, $2d(0,0.5,0.5)$, Fe, $2a(0,0,0)$, and O, $4i(x,0.5,z)$. Below 11 K the magnetic structure model has symmetry $P2_1$ with cell dimensions $a_M=a_N$, $b_M=2b_N$, $c_M=2c_N$, and $\beta_M=\beta_N$, and $M_y=M_z=0$. R_p is the residual, and R_{wp} is the weighted residual.

| Space Group | 4 K | 17 K |
|--------------------------|------------|-------------|
| | $C2/m$ | $R\bar{3}m$ |
| a (Å) | 11.5739(2) | 3.03134(1) |
| b (Å) | 3.03979(2) | |
| c (Å) | 5.98156(8) | 17.1724(1) |
| β (deg) | 154.341(1) | |
| V (Å ³) | 91.125(2) | 136.657(1) |
| Cu B (Å ²) | 0.25(2) | 0.28(1) |
| Fe B (Å ²) | 0.24(1) | 0.25(1) |
| M_x (μ_B) | 4.17(3) | |
| O x | 0.8938(1) | |
| O z | 0.6090(3) | 0.10724(1) |
| R_p (%) | 6.51 | 6.48 |
| R_{wp} (%) | 9.26 | 8.40 |
| χ^2 | 1.97 | 1.79 |

changed across T_N . The low-temperature magnetic structure was modeled using an orthorhombic unit cell of $\sqrt{3}a_h \times 2a_h \times 2c_h$ which is composed of six layers with four spins in each layer.²⁴ However, we found that the magnetic structure at 4 K can be determined based on a monoclinic unit cell (magnetic space group $P2_1$) derived from doubling the nuclear unit cell along the b and c directions [Fig. 1(d)]. Selected results of the General Structure Analysis System refinements²⁵ of NPD data are shown in Table I. The magnetic moment directions are nearly perpendicular to the Fe plane with an in-plane magnetic configuration consistent with the reported $\uparrow\uparrow\downarrow\downarrow$ spin structure. The magnetic moment of Fe^{3+} extrapolated to $T=0$ K is $(4.20 \pm 0.10)\mu_B$, slightly greater than $4.00\mu_B$ obtained from the previous neutron diffraction study,²⁴ but smaller than the spin moment $5\mu_B$ obtained from Mössbauer measurement.²⁶

Figure 3 shows the temperature dependence of the structural and magnetic properties of the CuFeO_2 system. Besides the well-characterized high- T hexagonal and low- T monoclinic phase, the system is somewhat complicated at temperatures between T_{N1} and T_{N2} . Despite the apparent asymmetrical broadening of the (110) and (102) peaks from synchrotron measurements, an accurate determination of the structure from the NPD refinements is difficult. This is because the temperature dependent incommensurate magnetic peaks result in an enlarged magnetic unit cell, leading to a modulated crystal structure due to the strong spin-lattice coupling. The full structural determination of the disordered phase may require an incommensurate structural description and thus is a subject of future investigations.

In order to understand the microscopic origin of the commensurate magnetic structure, we plot in Fig. 4 the detailed

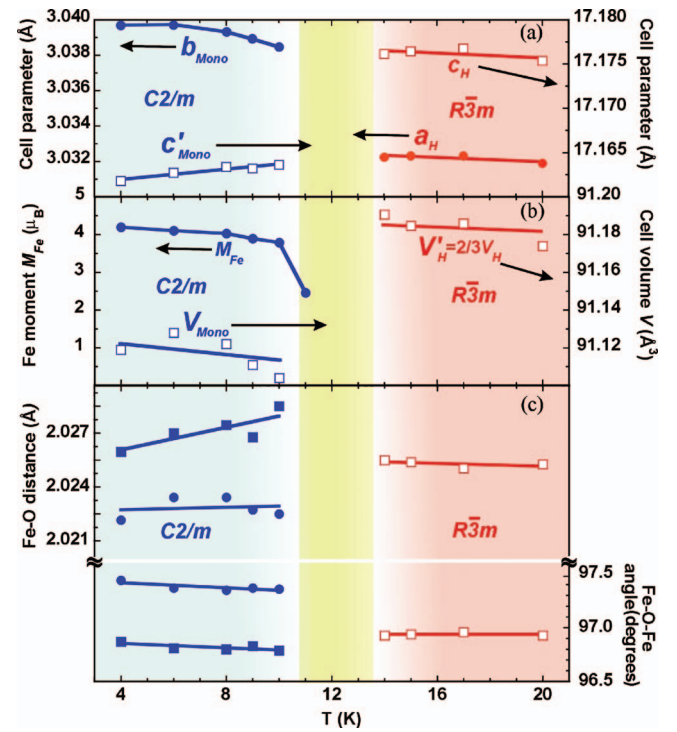


FIG. 3. (Color) Temperature dependence of (a) lattice parameters, (b) cell volume and Fe^{3+} moment, and (c) bonding distance and angles between Fe and O ions. All data derived from the NPD refinements.

structure of a layer of Fe^{3+} and the adjacent O^{2-} ions in the monoclinic phase at 4 K. Note that the hexagonal-to-monoclinic phase transition is caused by stretching the hexagonal unit cell along the b_H (b_M) axis, accompanied by a contraction along the c_H axis. As a consequence, the Fe-O-Fe bond angles (97.52°) and Fe-Fe distances (3.040 Å) between nearest-neighbor Fe ions are enlarged along the b axis at 4 K, while they are almost unchanged (96.82° and 3.029 Å, respectively) along the other two directions at 120° from b . This is different from those (96.89° and 3.031 Å,

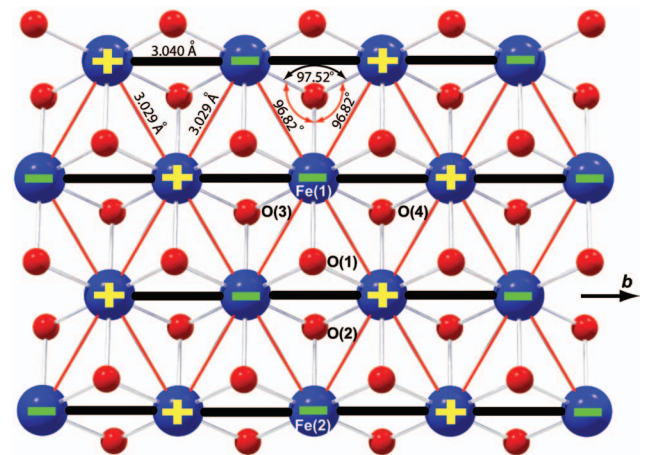


FIG. 4. (Color) Local structure in the layered Fe plane with two adjacent O planes. The Fe and O ions are presented in large (blue) and small (red) balls.

respectively) in the hexagonal phase. According to the Goodenough-Kanamori-Anderson rules, a larger covalent bonding angle between transition metal and oxygen ions would lead to a stronger AF coupling. Such an enhanced AF interaction would then induce AF coupled spin chains in the b direction. However, the zigzag AF couplings between the AF spin chains are still frustrated. Then, we considered another effect caused by the monoclinic lattice distortion; that is, shortening of the O(1)-O(2) distance [2.665 Å between O(1) and O(2); 2.688 Å between O(1) and O(3 or 4)] (see Fig. 4). In the $\uparrow\uparrow\downarrow$ spin structure of CuFeO_2 , the next-nearest-neighbor interaction in the direction perpendicular to the b axis is ferromagnetic (FM) at all Fe sites, as illustrated in Fig. 4. The shortening of the O(1)-O(2) distance may enhance the FM Fe(1)-O(1)-O(2)-Fe(2) exchange interaction. Thus, the monoclinic lattice distortion stabilizes the $\uparrow\uparrow\downarrow$ spin structure. A similar enhancement of the third-nearest-neighbor interaction caused by the shortening of O-O distance has been discussed in perovskite rare-earth manganites (e.g., HoMnO_3) in which the up-up-down-down spin structure is realized.²⁷

The discovery of two successive structural phase transi-

tions coupled with incommensurate and commensurate AF transitions suggests the presence of strong spin-lattice coupling. The symmetry-lowering structural transition from the high-symmetry hexagonal to the monoclinic structure is probably due to the bond order induced by magnetoelastic coupling in the partially disordered phase.²⁸ The simultaneous occurrence of a noncollinear spin structure, additional incommensurate structural modulation, and electric polarization, all induced by magnetic field, indicates that the multiferroic effect is determined by the spin configuration as well as the corresponding structural modifications.

Note added in proof. Recently, we became aware of the paper by Terada *et al.*,²⁹ which also reports the observation of a lattice distortion below T_{N2} .

We are grateful to B. Chakoumakos and V. O. Garlea for useful discussions. This work is supported by the U.S. DOE Grants No. DE-FG02-05ER46202 and DE-AC05-00OR22725 with UT/Battelle LLC. Use of the Advanced Photon Source was supported by the U.S. Department of Energy, Office of Science, Office of Basic Energy Sciences, under Contract No. W-31-109-Eng-38.

-
- ¹T. Kimura, T. Goto, H. Shintani, K. Ishizaka, T. Arima, and Y. Tokura, *Nature* (London) **426**, 55 (2003).
- ²N. Hur, S. Park, P. A. Sharma, J. S. Ahn, S. Guha, and S.-W. Cheong, *Nature* (London) **429**, 392 (2004).
- ³T. Lottermoser, T. Lonkai, U. Amann, D. Hohlwein, J. Ihlinger, and M. Fiebig, *Nature* (London) **430**, 541 (2004).
- ⁴G. H. Wannier, *Phys. Rev.* **79**, 357 (1950).
- ⁵P. W. Anderson, *Phys. Rev.* **102**, 1008 (1956).
- ⁶M. F. Collins and O. A. Petrenko, *Can. J. Phys.* **75**, 605 (1997).
- ⁷S.-H. Lee, D. Louca, H. Ueda, S. Park, T. J. Sato, M. Isobe, Y. Ueda, S. Rosenkranz, P. Zschack, J. Íñiguez, Y. Qiu, and R. Osborn, *Phys. Rev. Lett.* **93**, 156407 (2004).
- ⁸O. P. Vajk, M. Kenzelmann, J. W. Lynn, S. B. Kim, and S.-W. Cheong, *Phys. Rev. Lett.* **94**, 087601 (2005).
- ⁹I. E. Dzyaloshinskii, *Sov. Phys. JETP* **10**, 628 (1960).
- ¹⁰D. N. Astrov, *Sov. Phys. JETP* **11**, 708 (1960).
- ¹¹H. Katsura, N. Nagaosa, and A. V. Balatsky, *Phys. Rev. Lett.* **95**, 057205 (2005).
- ¹²A. P. Ramirez, *Annu. Rev. Mater. Sci.* **24**, 453 (1994).
- ¹³O. Nagai, in *Frustrated Spin Systems*, edited by H. T. Diep (World Scientific, Singapore, 2004), p. 59.
- ¹⁴S. Nakatsuji, Y. Nambu, H. Tonomura, O. Sakai, S. Jonas, C. Broholm, H. Tsunetsugu, Y. Qiu, and Y. Maeno, *Science* **309**, 1697 (2005).
- ¹⁵N. Terada, T. Kawasaki, S. Mitsuda, H. Kimura, and Y. Noda, *J. Phys. Soc. Jpn.* **74**, 1561 (2005).
- ¹⁶H. Kawamura, *J. Phys.: Condens. Matter* **10**, 4707 (1998).
- ¹⁷S. Mitsuda, M. Mase, T. Uno, H. Kitazawa, and H. Katori, *J. Phys. Soc. Jpn.* **69**, 33 (2000); N. Terada, S. Mitsuda, T. Fujii, K. Soejima, I. Doi, H. Katori, and Y. Noda, *ibid.* **74**, 2604 (2005).
- ¹⁸S. Mitsuda, N. Kasahara, T. Uno, and M. Mase, *J. Phys. Soc. Jpn.* **67**, 4026 (1998).
- ¹⁹Y. Ajiro, T. Asano, T. Takagi, M. Mekata, H. Katori, and T. Goto, *Physica B* **201**, 71 (1994).
- ²⁰O. A. Petrenko, G. Balakrishnan, M. R. Lees, D. M. Paul, and A. Hoser, *Phys. Rev. B* **62**, 8983 (2000).
- ²¹T. Kimura, J. C. Lashley, and A. P. Ramirez, *Phys. Rev. B* **73**, 220401(R) (2006).
- ²²S. Mitsuda, H. Yoshizawa, N. Yaguchi, and M. Mekata, *J. Phys. Soc. Jpn.* **60**, 1885 (1991).
- ²³S. Mitsuda, M. Mase, K. Prokes, H. Kitazawa, and H. Katori, *J. Phys. Soc. Jpn.* **69**, 3513 (2000).
- ²⁴M. Mekata, N. Yaguchi, T. Takagi, S. Mitsuda, and H. Yoshizawa, *J. Magn. Magn. Mater.* **104**, 823 (1992).
- ²⁵A. C. Larson and R. B. Von Dreele, Report No. LAUR-86-748, Los Alamos National Laboratory, Los Alamos, NM 87545, 1990 (unpublished).
- ²⁶A. H. Muir, Jr. and H. Wiedersich, *J. Phys. Chem. Solids* **28**, 65 (1967).
- ²⁷T. Kimura, S. Ishihara, H. Shintani, T. Arima, K. T. Takahashi, K. Ishizaka, and Y. Tokura, *Phys. Rev. B* **68**, 060403(R) (2003).
- ²⁸O. Tchernyshyov, R. Moessner, and S. L. Sondhi, *Phys. Rev. Lett.* **88**, 067203 (2002); O. Tchernyshyov, O. A. Starykh, R. Moessner, and A. G. Abanov, *Phys. Rev. B* **68**, 144422 (2003).
- ²⁹N. Terada, S. Mitsuda, H. Ohsumi, and K. Tajima, *J. Phys. Soc. Jpn.* **75**, 023602 (2006).